Journal of Asian Earth Sciences
Manuscript Draft

Manuscript Number: JAES-D-18-00747

Title: U-Pb ZIRCON GEOCHRONOLOGY OF INTRUSIVE ROCKS FROM AN EXOTIC BLOCK IN THE LATE CRETACEOUS - PALEOCENE TARAKLı FLYSCH (SAKARYA TERRANE, TURKEY): CONSTRAINTS ON THE TECTONICS OF THE INTRAPONTIDE SUTURE ZONE

Article Type: Research Paper

Keywords: Permian granitoids; slide-block; foredeep, U/Pb zircon geochronology; Taraklı Flysch; Turkey.

Abstract: In the Boyalı area (northern Anatolia), a thick succession of the Early Maastrichtian - Middle Paleocene Taraklı Flysch crops out. The Taraklı Flysch represents a foredeep deposit sedimented during the final stage of collision between Sakarya and Istanbul-Zonguldak continental margins, that developed as consequence of the closure of the Intrapontide oceanic basin.
The top of the Taraklı Flysch is characterized by a level of slide-block in shaly-matrix lithofacies that can be considered as a fast catastrophic event predating the closure of the basin and its deformation. This level consists of slide-blocks sourrounded by monomict pebbly-mudstones and pebbly-sandstones. Among the slide-blocks, the biggest one consists of quartz-monzonites and leucocratic granodiorites of Late Permian age (260.8 ± 2.2 Ma) dated by zircon LA-ICP-MS method. By comparison with the regional data, the source area of these granitoids can be identified in the Istanbul-Zonguldak terrane. This evidence suggests a new picture for the paleogeographic setting of the ultimate stage of the continental collision between the Istanbul-Zonguldak and Sakarya continental margins. In this scenario the coarse-grained deposits of the Taraklı Flysch are supplied by an orogenic wedge, consisting of oceanic units topped by the Istanbul-Zonguldak terrane. This orogenic wedge represents the northern side of the foredeep, where the southern one is represented by the still undeformed Sakarya continental margin.

***Highlights (for review)**

Highlights

- The Early Maastrichtian – Middle Paleocene Taraklı Flysch is a foredeep deposit sedimented during the continental collision between Sakarya and Istanbul-Zondulgak continental margins.
- The stratigraphic top of the Taraklı Flysch is represented by a "slide-blocks in shaly-matrix" lithofacies.
- The Permian magmatic age of the felsic plutonic rocks from a slide-block found at the top of the Taraklı Flysch is determined by U-Pb geochronology on zircon crystals.
- The source area of the slide-block of Permian felsic plutonic rocks is identified in the Istanbul-Zondulgak continental margin.
- The geodynamic setting of the foredeep during the sedimentation of the Taraklı Flysch is reconstructed.

U-Pb ZIRCON GEOCHRONOLOGY OF INTRUSIVE ROCKS FROM AN EXOTIC BLOCK IN THE LATE CRETACEOUS - PALEOCENE TARAKLı FLYSCH (SAKARYA TERRANE, TURKEY): CONSTRAINTS ON THE TECTONICS OF THE INTRAPONTIDE SUTURE ZONE

Maria Di Rosa[a,b], Federico Farina[c], Michele Marroni[a,d], Luca Pandolfi[a,d], M. Cemal Göncüoğlu[e], Alessandro Ellero[d], Giuseppe Ottria[d]

a Dipartimento di Scienze della Terra, Università di Pisa, Italy

b Dipartimento di Scienze della Terra, Università di Firenze, Italy

c Department of Earth Sciences, University of Geneva, Switzerland

d Istituto di Geoscienze e Georisorse, CNR, Pisa, Italy

e Department of Geological Engineering, Middle East Technical University, Ankara, Turkey.

==

* CORRESPONDING AUTHOR:

DR. MARIA DI ROSA,

DIPARTIMENTO DI SCIENZE DELLA TERRA,

UNIVERSITÀ DI PISA, VIA S. MARIA, 53

56126 PISA, ITALY.

E-MAIL: maria.dirosa@unifi.it

ABSTRACT

In the Boyalı area (northern Anatolia), a thick succession of the Early Maastrichtian - Middle Paleocene Taraklı Flysch crops out. The Taraklı Flysch represents a foredeep deposit sedimented during the final stage of collision between Sakarya and Istanbul-Zonguldak continental margins, that developed as consequence of the closure of the Intrapontide oceanic basin.

The top of the Taraklı Flysch is characterized by a level of slide-block in shaly-matrix lithofacies that can be considered as a fast catastrophic event predating the closure of the basin and its deformation. This level consists of slide-blocks sourrounded by monomict pebbly-mudstones and pebbly-sandstones. Among the slide-blocks, the biggest one consists of quartz-monzonites and leucocratic granodiorites of Late Permian age (260.8 ± 2.2 Ma) dated by zircon LA-ICP-MS method. By comparison with the regional data, the source area of these granitoids can be identified in the Istanbul-Zonguldak terrane. This evidence suggests a new picture for the paleogeographic setting of the ultimate stage of the continental collision between the Istanbul-Zonguldak and Sakarya continental margins. In this scenario the coarse-grained deposits of the Taraklı Flysch are supplied by an orogenic wedge, consisting of oceanic units topped by the Istanbul-Zonguldak terrane. This orogenic wedge represents the northern side of the foredeep, where the southern one is represented by the still undeformed Sakarya continental margin.

KEY-WORDS

Permian granitoids, slide-block, foredeep, U/Pb zircon geochronology, Taraklı Flysch, Turkey.

1. INTRODUCTION

Foreland basins represent a first-order tectonic element in the framework of collisional belts (e.g., Allen et al., 1986; DeCelles and Gilles, 1996). They originate during the first stage of collision when a passive margin collides with an active continental margin after the closure of an oceanic basin by subduction/obduction processes. One of the depozones of the foreland basin is represented by the foredeep, i.e. an elongate, deep sea-floor depression generally filled by turbidites, sometime associated to debris flows and slide deposits, which are supplied by the advancing orogenic wedge or, to a lesser extent, by the peripheral bulge. In addition, turbidites supplied by extrabasinal, distal domains and transported parallel to the front of the advancing wedge can be also deposited in the foredeep.

The characteristics of these sediments provide useful insights for the reconstruction of the history of the collisional belt through time and space (e.g. Dickinson, 1988; Fedo et al., 2003; Carrapa, 2010). In this frame, the coarser grained deposits, like the slide-blocks, can be used to retrieve direct information on the source areas that sorrounded the foredeep, providing valuable paleogeographic constraints.

The tectonic setting of Turkey (Fig. 1) can be described as a puzzle of amalgated continental microplates separated by ophiolite-bearing sutures derived by the closure of different branches of oceanic basins whose ages range from Late Neoproterozoic to Late Cretaceous (e.g. Göncüoğlu et al., 1997; Okay and Tüysüz, 1999; Moix et al., 2008 and quoted references). The closure of these oceanic branches by subduction/obduction processes is followed by various stages of continental collision leading to the development of foredeeps that change in time and in space their shape, infilling mechanism and sediment types. One of these sutures is the Intrapontide suture (IPS) zone, located in the northern Turkey between the Sakarya (SK) and Istanbul-Zonguldak (IZ) continental terranes. In this suture zone, the foredeep deposits are represented by the Late Cretaceous - Middle Paleocene Taraklı Flysch deposited at the top of the SK terrane during the final stage of the continental collision between the SK and IZ continental margins (Catanzariti et al., 2013 and quoted references). Until now, the scenario during this late stage collision has not been reconstructed in detail, because the original tectonic setting of the IPS zone has been strongly reworked by the active strike-slip North Anatolian Shear Zone (NASZ; Şengör et al., 2005; Ellero et al., 2015a). However, useful information on this scenario can be obtained by the analysis of the coarse-grained deposits occurring in the Taraklı Flysch, these can shed light on the nature of the domains that surrounded the foredeep during the deposition of the Taraklı Flysch.

In this paper, we have studied the petrography and determined the U-Pb age of plutonic rocks found as an exotic block in the Late Cretaceous - Paleocene Taraklı Flysch from Boyalı area (central Anatolia). In order to identify the source area of this intrusive body, its age and first-order petrographic characteristics are compared with other plutonic rocks described in both the SK and IZ terranes. At last, the resulting evidence, together with a review of the main stratigraphic features of the Taraklı Flysch, allows a better understanding on the final stage of the continental collision, as, for instance, the features of the orogenic wedge at the border of the foredeep.

2. THE INTRAPONTIDE SUTURE ZONE: TECTONIC BACKGROUND

The tectonic setting of Turkey (Fig. 1) is characterized by several Paleo- and Neotethys suture zones that are distributed around several continental terranes of both Gondwana- and Laurasia-origin (Şengör and Yilmaz, 1981; Okay, 1986; Robertson, 2002; Moix et al., 2008; Göncüoğlu, 2010; Plunder et al., 2013; van Hinsbergen et al., 2016). This tectonic setting is the result of a long-lived geodynamics history of Mesozoic age and is originated by the complex interplay between small continental microplates and wide oceanic areas, all located between the continental margins of two megaplates, the Gondwana to the south and the Laurasia to the north (Stampfli and Borel, 2002; Stampfli and Kozur, 2006). These oceanic areas were originated and subsequently destroyed by subduction and obduction processes leading to multiple continental collisional events whose record is partially preserved in the suture zones.

The northernmost suture zone preserved in Turkey IPS zone, an east-west trending assemblage of deformed and metamorphic continental and oceanic units running from the Aegean coast to the central Anatolia (e.g. Şengör and Yılmaz, 1981; Okay and Tüysüz, 1999; Göncüoğlu et al., 2008; Hippolyte et al., 2010, 2016; Marroni et al., 2014; Frassi et al., 2016; Okay et al., 2017). The units of IPS zone are thrust by the IZ continental terrane and both are, in turn, thrust over the SK continental terrane. However, the pristine tectonic relationships of these units with the continental terranes are strongly modified since Early Eocene by the brittle tectonics related to the NASZ (Ottria et al., 2017 and references therein).

The oceanic units occurring in the IPS zone indicate that a large oceanic area, known as the Intra-Pontide Ocean basin, existed since the Trias between the SK and the IZ continental margins (Şengör and Yılmaz, 1981; Göncüoğlu et al., 1987, 2008, 2012, 2014; Yılmaz, 1990; Göncüoğlu and Erendil, 1990; Robertson et al., 1991; Okay et al., 1996; Yılmaz et al., 1997;

Okay and Tüysüz, 1999; Okay, 2000; Robertson and Ustaömer, 2004; Akbayram et al., 2012; Marroni et al., 2014; Frassi et al., 2018). The SK and IZ margins were part of two microplates which were separated by the Intra-Pontide Ocean basin, a large oceanic area that was progressively closed by subduction and obduction events as proven by the occurrence of oceanic units showing HP/LT metamorphism of Late Jurassic age (Daday, Saka and Domuz Dag Units; Okay et al., 2006, 2013; Marroni et al., 2014; Aygül et al., 2015a; Frassi et al., 2018). These units are associated to non-metamorphic Late Jurassic ophiolites and ophiolite-bearing sedimentary mélanges of Late Cretaceous age (Arkotdag and Kızılırmak mélanges; Tokay, 1973, Göncüoğlu et al., 2012, 2014; Çelik et al., 2016). Further evidence supporting the closure of the Intra-Pontide Ocean basin are provided by the remnants of volcanis arc of Late Cretaceous age, today preserved as tectonic units within the IPS zone (Ellero et al., 2015b; Aygül et al., 2015b).

The tectonic units from the IPS zone are thrust over the SK continental terrane that consists of a Variscan continental basement associated with a strongly deformed and metamorphosed Triassic subduction complex (i.e. the Karakaya Complex; Okay et al., 2002; Okay and Göncüoğlu, 2004; Sayit and Göncüoğlu, 2013). This basement is unconformably covered by Early Jurassic to Late Cretaceous, continental to deep-marine sedimentary succession passing upward to turbidites (here reported as Taraklı Flysch), regarded as a foredeep deposits ranging in age from Early Maastrichtian to Middle Paleocene (Catanzariti et al., 2013).

In turn, the IZ terrane includes a Neoproterozoic basement (e.g. Ustaömer and Rogers, 1999) unconformably overlain by a very thick sedimentary sequence whose age spans from Ordovician to Carboniferous (e.g. Görür et al., 1997). Such a Paleozoic sequence is unconformably overlain by a thick sequence of Late Permian-Triassic continental clastic deposits topped by Middle to Late Jurassic carbonate deposits, which are covered by Late Cretaceous-Paleocene turbidite deposits interleaved with andesitic volcanic flows (e.g. Dizer and Meriç, 1983; Aydın et al., 1986).

In this framework, the Taraklı Flysch deserves special attention mainly because it allowed assigning the ultimate stage of collision between IZ and SK terranes to the Middle Paleocene (Catanzariti et al., 2013).

3. THE TARAKLI FLYSCH IN THE BOYALı AREA

3.1 Geological setting

The studied section of the Taraklı Flysch is located in the Boyalı area, northern Anatolia along the Akçay Valley between the Bahçecik and Boyalı Villages (Fig. 2a). This valley shows an east-west trend and its northern flank is delimited by the Aylı Dağ Mountain.

In this area the tectonic setting is dominated by the deformation related to the NASZ which affected a tectonic stacking characterized by three imbricate units belonging to the IPS zone, namely the ophiolite Aylı Dağ Unit (Göncüoğlu et al., 2012), the Arkot Dağ Mélange (Göncüoğlu et al., 2014) and the Daday Unit (Frassi et al., 2018), that are thrust all together over the SK terrane (Catanzariti et al., 2013; Ellero et al., 2015a) (Fig. 2a and b). In this area, the SK terrane display a stratigraphic log that includes continental- to shallow-marine Early Jurassic clastic rocks that are disconformably topped by the Middle Jurassic to Early Cretaceous neritic limestones (Altıner et al., 1991). The neritic limestones are unconformably overlain by the Early to Late Cretaceous pelagic limestones showing a transition to turbidite deposits of the Taraklı Flysch ranging in age from Early Maastrichtian to Middle Paleocene.

South of Boyalı village (Fig. 2a), the Taraklı Flysch is imbricated with slices of the Tafano Unit (Ellero et al., 2015b) probably as result of the strike-slip tectonics of the NASZ. The Tafano Unit consists of a Late Cretaceous sequence including a volcanic complex covered by sedimentary succession. The volcanic rocks, that display basaltic and basaltic-andesitic compositions with sub-alkaline affinities, are associated with volcaniclastic deposits evolving to late Santonian-middle Campanian marly-calcareous turbidites.

In addition, a small klippe of the IZ terrane consisting of Devonian deposits has been identified between two NE-SW striking strike-slip faults at the top of the Arkot Dağ Mélange, west of the Ayli Dağ Mountain (Fig. 2a).

The relationships among these units are sealed by the Late Paleocene-Eocene deposits of the Safranbolu-Karabuk Basin (Fig. 2a) that widely crop out in the in the western part of the Akçay Valley. Thus, the relationships between the tectonic units of the IPS zone and the SK and IZ terranes can be regarded as the result of the pre-Eocene tectonic events.

3.2 Stratigraphic features

The stratigraphy of the Taraklı Flysch (Fig. 3a) has been reconstructed by Catanzariti et al. (2013) in the sections cropping out along the northern side of the Akçay Valley, between the Bahçecik and Boyalı Villages and along the Boyalıçay Valley. In this study we have expanded the field survey of Catanzariti et al. (2013), mapping the western extent of the Akçay Valley (Fig. 2c).

The thickness of the Taraklı Flysch is at least 700 m and shows a thickening and coarsening upward evolution (Fig. 3a). According to Catanzariti et al. (2013) it can be divided in five different lithofacies that, from the bottom to the top, are: "thin-bedded turbidites", "medium-grained arenites", "conglomerates", "calcareous coarse-grained turbidites" and "slide-blocks in shaly-matrix" lithofacies (Fig. 3b). In the study area the "calcareous coarse-grained turbidites" facies is not present while the conglomerates facies is well developed.

The thin-bedded turbidites facies is, at least, 400 m thin to medium beds of medium- to fine-grained arenites and coarse-grained siltites (Fig. 3c) . These strata are well graded low density turbidites (F9a facies of Mutti, 1992) and current ripples and sinusoidal lamina are common.

The medium-grained arenites lithofacies is characterized by up to 70 m thick sequence of turbidites represented by 0.4-2 m thick beds of amalgamated medium- to fine-grained arenites (Fig. 3d). These strata are characterized by a massive structure and they can be compared with the F8 facies of Mutti (1992). The bottom surface of these strata is characterized by sole marks and by the common presence of organic matter.

A thick level of well rounded clast- to matrix-supported conglomerates (F3 facies of Mutti, 1992) characterizes the medium part of the Taraklı Flysch (Fig. 3e). These strata are associated with coarse-grained high density turbidity current deposits. Thick to medium beds without internal structures and with poor sorting are the most common facies. The “conglomerates” lithofacies is characterized by granitoids-dominated composition of the pebbles while the carbonatic clasts are rare. These beds, derived from high density erosive flows probably connected to a coarse-grained river-delta systems.

The upper part of the succession, which in the studied area is more than 300 m thick, is dominated by slide-blocks embedded in a fine grained-matrix (Fig. 3f). The matrix of this lithofacies is characterized by varicolored mainly shaly to silty deposits. The slide-blocks, usually with lenticular shapes, have variable composition and sizes ranging from metresized boulder up to more than 100 m-thick blocks. Even if the primary relationships between the slide-blocks and the surrounding matrix are always tectonized, their emplacement due to submarine landslides for these blocks is suggested by synsedimentary deformation structures recognized in the sediments around the blocks and by slide-block-derived monomict pebbly-mudstones and pebbly-sandstones that are present around several slide-blocks. The slide-blocks are mainly granitoids (Fig.3g), orthogneisses, metagabbros/amphibolites, Jurassic carbonatic turbidites as well as Ordovician quartzarenites, black shales, crinoidal and brachiopod-bearing Devonian-Carboniferous limestones and probably Triassic red quartz-arenites which are typically derived from the IZ terrane. As indicated in the geological scheme of Fig. 2a, the granitoids blocks are the most common and those cropping out between the villages of Boyalı and Bahcecik and, to a lesser extent between Boyalı and Bayar[illegible]en villages, can be mapped at the 1:10.000 scale. Within the individual slide-blocks of plutonic rocks primary relationships among different magmatic lithofacies can be recognized. These slide-blocks can be regarded as “exotic” as similar lithologies have not been found in the units cropping out in the sorrounding area. We have sampled a large intrusive exotic block that, as illustrated in the geological map of Fig. 2c, covers an area of ca. 9 km^2. In the next paragraphs the textural features of this block as well as its zircon U-Pb age will be presented and discussed in relationship to granitoids occurring in various terranes surrounding the IPS zone.

4. ZIRCON SEPARATION AND U-Pb GEOCHRONOLOGY

Zircons were extracted from their host rocks at the University of Geneva (Switzerland) by standard crushing, gravimetric- and magnetic-separation techniques. Approximately 200 zircon crystals were selected from each hand sample. These crystals were hand-picked under a binocular microscope and mounted in epoxy resin. The mounts were polished to expose the crystal interior domains and imaged by cathodoluminescence using a JEOL JSM-7001F Schottky scanning electron microscope at the University of Geneva.

In-situ zircon U-Pb isotope analysis were performed at the Institute of Earth Sciences of the University of Lausanne (Switzerland) using a Thermo ELEMENT XR sector field ICP-MS coupled with a Resolution 193 nm Excimer laser ablation system. Data were acquired in time-resolved, peak-jumping, pulse-counting mode utilizing a routine where 30 seconds of background measurement were followed by 30 seconds of sample ablation. Laser induced fractionation of Pb and U was minimized during analysis by employing a soft ablation regime using a repetition rate of 5 Hz and an energy density of ~3 J/cm^2 per pulse. Laser spot sizes were 30 µm. The measurement protocol and the parameters of mass spectrometer optimization follow Ulianov et al. (2012). Laser-induced elemental fractionation and instrumental mass discrimination were corrected by normalization to the reference zircon GJ-1. To test the accuracy and external reproducibility of the obtained age data, the Plešovice reference zircon (Sláma et al., 2008) was measured after every ~ 8 unknowns and the data are presented in Table 1. The Plešovice secondary standard gave a weighted mean age of 337.5 ± 0.6 Ma (2SD, n = 21; MSWD = 0.66). The calculated age is consistent, within uncertainty, with the ID-TIMS value reported by Sláma et al. (2008). All raw data from Lausanne was processed using the LAMTRACE software package (Jackson, 2008) and no common Pb correction was applied due to the presence of trace ^{204}Hg in the Ar gas. Common Pb was dealt with by monitoring ^{201}Hg, $^{204}(Hg+Pb)$ as well as

(^{204}Pb+^{204}Hg)/^{206}Pb ratios. The homogeneity of the ablated material was confirmed by monitoring the ^{206}Pb/^{238}U and ^{207}Pb/^{235}U vs. time spectra, and fluctuations in these ratios were interpreted to represent mixing between different age domains within the crystals. Spectra with mixed domains were subsequently discarded.

5. INTRUSIVE ROCKS IN THE BOYALı AREA

5.1 Field data and petrography

We have sampled a large-block of granitoids that, as illustrated in the geological map of Fig. 2b, occurs as a square body and it is cut, in its northern side, by an E-W trending strike-slip fault. The granitoids are well exposed along the Akçay river where two different facies were recognized (Fig. 4a).

The main, melanocratic facies (Fig. 4b) is located in the upper level of the block and consists of medium-grained quartz-monzonites (Fig. 4c) with crystal of amphibole representing the dominant rock-forming phase forming up to ca. 50 vol% of the rock assemblage. The quartz-monzonites also contains widespread crystals of quartz, titanite as well as primary iron-rich epidote and a minor amount of chlorite replacing former biotite crystals. Other common accessory phases are apatite, magnetite and zircon. No preferred orientation of the minerals has been observed in these rocks. The most voluminous facies is intruded by a second leucocratic unit (Fig. 4d) that occurs in the lower level of the slide-block. This second facies is made of coarse-grained leucocratic granodiorite (Fig. 4e) with crystals reaching up to 5 cm of K-feldspar, quartz and plagioclase. Mirmekitic textures are common in some of the analyzed thin sections. Biotite is the main ferromagnesian phase in the rock forming less than 5 vol% of the granodiorites and biotite crystals are pervasively altered to iron-rich chlorites (i.e. chamosite). Accessory phases are titanite crystals, reaching up to 1 mm in size, primary iron-rich epidote (i.e. pistacite), apatite and zircon. In thin section, both lithofacies are cross-cut by different generations of calcite veins and the plagioclase in the quartz-monzonites is commonly pervasively altered to sericite. Dikes of the leucocratic granodiorites cut the quartz-monzonites (Fig. 4f) whereas the latter form enclaves that are recognized along the contact zone between the two units. Finally, both the lithotypes are cross-cut by fine-grained aplitic dikes.

5. 2 Zircon texture and U-Pb geochronology

Zircon were extracted from three samples (Fig. 5). Two samples of the quartz-monzonites (i.e. TC316a and TC316b) and one from the leucocratic granodiorites (TC319). Zircon crystals from both lithofacies are subhedral to euhedral and reach up to 350 µm in length. Under cathodoluminescence (hereafter CL), most of the grains from the quartz-monzonites are characterized by the occurrence of CL-dark homogeneous or faintly zoned centres surrounded by fine-scale oscillatory zoned rims. The centres commonly exhibit evidence of resorption, they can be fractured and occasionally metamictic (Fig. 5). Most of zircon grains from the leucocratic granodiorites exhibit complex core-to-rim growth zoning with common local intermediate resorption features that allows distinguish centres and rims (Fig. 5). A subset of zircon crystals from both rock-types are homogeneous under CL, either bright or dark.

Seventy-two zircon crystals were dated by LA-ICP-MS U-Pb analysis. The complete dataset is provided in Table 1. In Fig. 6, Concordia diagrams and weighted average plots are shown. The analyses performed on both centres and rims yield apparent spot ages that vary from

270 to 232 Ma, with most of the data forming a cluster at ca 260 Ma. Most of the spot analyses are discordant and only twenty-three analyses passed the <10% discordancy test (Conc.(%) in Tab.1). The two samples analysed for the quartz-monzonites yielded weighted average $^{206}Pb/^{238}U$ ages of 261.0 ± 1.6 Ma (n=16, MSWD = 0.5) and 258.3 ± 2.1 Ma (n=15, MSWD = 1.2). Zircon spot ages from the leucocratic granodiorites are more scattered giving a weighted average $^{206}Pb/^{238}U$ age of 256.8 ± 2.8 Ma (n=18, MSWD = 3.1). These three calculated ages are the same within error, a weighted mean $^{206}Pb/^{238}U$ age determined considered only the sub-concordant spot analyses for the three rocks considered together yielded an age of 260.8 ± 2.2 Ma. This is considered to be the age of emplacement of the intrusive body.

6. DISCUSSION

6.1 Occurrence of slide-blocks of Late Permian granitoids in the Taraklı Flysch

The succession of the Taraklı Flysch cropping out in the Boyalı area (Fig. 3a) shows all the features of syn-tectonic sedimentation in a foredeep environment with a clear thickening and coarsening upward evolution from thin-bedded turbidites to medium-grained arenites and calcareous coarse-grained turbidite lithofacies (Catanzariti et al., 2013). This succession ends with a level of slide-blocks in shaly-matrix lithofacies, that can be considered as the result of a fast and catastrophic sedimentary event that predates the closure of the basin and its deformation. This catastrophic event originated by the instability of the front of the orogenic wedge probably triggered by earthquakes induced by the underthrusting of a lower plate with rugged morphology, as detected in modern and fossil foredeep and trench deposits (Festa et al., 2010 and quoted references.). The slide-blocks are sourrounded by monomict pebbly-mudstones and pebbly-sandstones whereas the sediments around show synsedimentary deformation structures. Among the different slide-blocks, the largest one is the studied zoned pluton with other petrographically similar blocks of minor dimensions cropping out next to it (Fig. 2c). These lines of evidence suggest that all the slide-blocks derived from a source area that was located close to the foredeep where the Taraklı Flysch sedimented. Thus, this source area can be identified either in the front of the advancing orogenic wedge or, alternatively, in the peripheral bulge, being these areas the only ones that are able to provide coarse-grained deposits in the upper part of the Taraklı Flysch. In the first hypothesis, the source area of the slide-blocks of granitoids is represented by IZ terrane, whereas in the second one the same role is played by the SK terrane.

6.2 Felsic plutonic rocks in the SK and IZ terranes

Undeformed plutonic rocks of Paleozoic age occur in both the SK and IZ terranes (Okay and Topuz, 2017). In the SK terrane, most of the unmetamorphosed granitoids are Devonian and crop out in the western part of the Sakarya zone as tectonic slices generally occurring within the Triassic subduction-accretion complexes (Karakaya Complex), (Okay et al., 1996, 2006; Aysal et al., 2012; Sunal, 2012). These intrusives, which are mainly granodiorites, monzogranites and monzodiorites show geochemical and petrographic features of continental arc magmas (Aysal et al., 2012). In the SK terrane Carboniferous - Early Permian granitoids are also common and widespread intruding the LP-HT metamorphic rocks cropping out in Eastern Pontide area. The U-Pb zircon ages of these granitoids, which exhibit both high-K I- and S-type signatures, range from 330 to 294 Ma (e.g., Ustaömer et al., 2012, 2013; Kaygusuz et al., 2012). Therefore the age of the intrusive rocks cropping out in the Sakarya terranes does not match with the age of the exotic block in the upper part of the Taraklı Flysch.

In the IZ terrane the Paleozoic sequence is continuous from Ordovician to Carboniferous with no intervening phases of magmatism or deformation (e.g., Görür et al., 1997; Özgül, 2012). The Ordovician sedimentary rocks are underlain by late Neoproterozoic granitoids (Ustaömer et al., 2005). The late Neoproterozoic granitoids as well as the Paleozoic sedimentary sequence were deformed and metamorphosed during the Carboniferous and were subsequently intruded by syn- and post-tectonic Late Carboniferous and Permian granitoids. These intrusive rocks show a wide range of ages from 309 to 235 Ma similar to the plutonic rocks described in the Strandja massif, Istanbul area and central Pontides (Ustaömer et al., 2005; Sunal et al., 2006; Sahin et al., 2014; Machev et al., 2015).

The Kürek granite, located in the IZ terrane only few kilometeres north of the studied exotic blocks in the Taraklı Flysch, has a Late Permian age of 262 ± 3 Ma (Okay et al., 2013) which overlaps with the age of the slide-block dated in this study. Therefore, this granitoid is considered to be the best candidate to represent the source of the slide-block in the Taraklı Flysch. It is worth noting that the Kürek granite and the slide-block also share similar petrographic features, with the former described by Okay et al. (2013) as a composite pluton consisting of hornblende-bearing diorites intruded by granites-granodiorites. The Kürek granites occurs at the top of the oceanic metamorphic units belonging to the IPS zone. This tectonic position suggests that the Kürek granites can be interpreted as a klippe belonging to the southernmost part of the IZ terrane, subsequently dislocated by the strike-slip tectonics related to the NASZ (Ellero et al., 2015a; Ottria et al., 2017).

6.3 Potential source area of slide-blocks in the Taraklı Flysch

The age and the petrography of the granitoids in the Taraklı Flysch match with those of granitoids derived from the IZ terrane. In fact, the IZ terrane differently from Sakarya, hosts Late Carboniferous to Permian granitoids, that crop out also in the Central Pontides. Klippes of IZ terrane occur 5 km north of the studied granitoids whereas another klippe of the IZ terrane bearing granitoids (Kürek granite) showing similar petrography and age occur about 25 Km northward. As previously stated, these klippes can be regarded the remnants of the southernmost part the IZ terrane, subsquently dismembered and isolated by the strike-slip tectonics.

Our data suggest that the slide-blocks of granitoids are derived from the advancing front of the IZ terrane located at the top of the orogenic wedge that bounded northward the foredeep where the Taraklı Flysch deposited. Another evidence in support of this hypothesis comes from the occurrence, in the uppermost part of the Taraklı Flysch of crinoidal and brachiopod-bearing Devonian-Carboniferous limestones and Triassic red quartzarenites. These lithologies are found in the IZ terrane. In this reconstruction, the IZ terrane can be regarded as a wide nappe that thrust over the IPS units reaching the rim of the foredeep. The slide-block of granitoids were then detached from the IZ terrane, emplaced by slide in the foredeep and interposed within the turbidites of the Taraklı Flysch. Conversely, the opposite side of the foredeep is represented by the SK continental margin, not still affected by deformation, that represents the source area for the thin-bedded turbidites of the Taraklı Flysch. A reconstruction of the depositional setting of the Taraklı Flysch is proposed in the Fig. 7.

7. CONCLUSION

The Taraklı Flysch from the Boyalı area is a turbidite deposit of Early Maastrichtian to Middle Paleocene age that sedimented in a foredeep during the ultimate stage of the collision between SK and IZ continental margins. The top of the Taraklı Flysch is characterized by a level of slide-blocks in shaly-matrix lithofacies, that can be considered as the fast catastrophic event that predates the closure of the basin and its deformation. This level consists of slide-blocks sourrounded by monomict pebbly-mudstones and pebbly-sandstones, whereas the sediments around show synsedimentary deformation structures. Among the slide-blocks, the largest one consists of intrusive rocks of Late Permian age by U/Pb geochronology. According to the available regional data, these “exotic” granitoids are derived from the IZ terrane, where Late Permian granites are widespread.

This evidence suggests a new picture for the paleogeographic setting in the Paleocene time, i.e. during the final stage of the continental collision between the IZ and SK continental margins (Fig. 7). In this picture the slide-blocks of granites are supplied from the advancing front of the IZ terrane located at the top of the orogenic wedge that bounded northward the foredeep. This wedge can be depicted as consisting of IPS units thrust by the IZ terrane. This picture is coherent with thrusting of the IZ terrane over the IPS units across the whole extension of the IPS zone during the continental collision and before the inception of the NASZ.

ACKNOWLEDGMENTS

The research has been funded by PRA of University of Pisa. This research benefits also by grants from Darius Project and PRIN 2010-11 projects (resp. M. Marroni). F. Farina wishes to acknowledge the financial support received fromthe European Union’s Horizon 2020 research and innovation program under the Marie Skłodowska-Curie grant agreement No 701494.

REFERENCES

Akbayram, K., Okay, A. I. , Satır, M., 2012. Early Cretaceous closure of the Intra-Pontide Ocean in western Pontides (northwestern Turkey). Journal of Geodynamics 65, 38-55.

Allen, P.A., Homewood, P., Williams, G.D., 1986. Foreland basins: an introduction. Foreland basins. International Association of Sedimentologists, Special Publication 8, 3-12.

Altıner, D., Koçyigit, A., Farinacci, A., Nicosia, U., Conti, M.A., 1991. Jurassic-Lower Cretaceous stratigraphy and paleogeographic evolution of the southern part of northwestern Anatolia. Geologica Romana 27, 13-80.

Aydın, M., Sahintürk, O., Serdar, H.S., Özçelik, Y., Akarsu, I., Üngör, A., Çokuğraş, R., Kasar, S., 1986. The geology of the area between Ballidağ and Çangaldağ (Kastamonu). Bulletin of the Geological Society of Turkey 29, 1-16.

Aygül, M., Okay, A.I., Oberhansli, R., Ziemann, M.A., 2015a. Thermal structure of low-grade accreted Lower Cretaceous distal turbidites, the Central Pontides, Turkey: insights for tectonic thickening of an accretionary wedge. Turkish Journal of Earth Sciences 24, 461-474.

Aygül, M., Okay, A.I., Oberhansli, R., Schmidt, A., Sudo, M., 2015b. Late Cretaceous infant intra-oceanic arc volcanism, the Central Pontides, Turkey: petrogenetic and tectonic implications. Journal of Asian Earth Sciences 111, 312-327.

Aysal, N., Ustaömer, T., Öngen, S., Keskin, M., Köksal, S., Peytcheva, I., Fanning, M., 2012. Origin of the Early-Middle Devonian magmatism in the Sakarya Zone, NW Turkey: Geochronology, geochemistry and isotope systematics. Journal of Asian Earth Sciences 45, 201-222.

Carrapa, B., 2010. Resolving tectonic problems by dating detrital minerals. Geology 38(2), 191-192.

Catanzariti, R., Ellero, A., Göncüoğlu, M.C., Marroni, M., Ottria, G., Pandolfi, L., 2013. The Taraklı Flysch in the Boyalı area (Sakarya Terrane, northern Turkey): implications for the tectonic history of the IntraPontide suture Zone. Comptes Rendus Geoscience 345, 454-61.

Çelik, Ö.F., Chiaradia, M., Marzoli, A., Özkan, M., Billor, Z., Topuz, G., 2016. Jurassic metabasic rocks in the Kızılırmak accretionary complex (Kargı region, Central Pontides, Northern Turkey). Tectonophysics 672/673, 34-49.

DeCelles, P. G. and Giles, K. A., 1996. Foreland basin systems. Basin research 8(2), 105-123.

Dickinson, W. R., 1988. Provenance and sediment dispersal in relation to paleotectonics and paleogeography of sedimentary basins. In: Dickinson, W.R. (Eds.), New Perspectives in Basin Analysis. Springer, New York, 3-25.

Dizer, A. and Meriç, E., 1983. Late Cretaceous-Paleocene stratigraphy in Northwest Anatolia. Maden Tetkik ve Arama Enstitutusu Dergisi 95/96, 149-163.

Festa, A., Pini, G. A., Dilek, Y., Codegone, G., 2010. Mélanges and mélange-forming processes: A historical overview and new concepts. International Geology Review, 52(10-12), 1040-1105.

Ellero, A., Ottria, G., Marroni, M., Pandolfi, L., Göncüoğlu, M.C., 2015a. Analysis of the North Anatolian Shear Zone in Central Pontides (northern Turkey): Insight for geometries and kinematics of deformation structures in a transpressional zone. Journal of Structural Geology 72, 124-141.

Ellero, A., Ottria, G., Sayit, K., Catanzariti, C., Frassi, C., Göncüoğlu, M.C., Marroni, M., Pandolfi, L., 2015b. Geological and geochemical evidence for a Late Cretaceous continental arc in the Central Pontides, Northern Turkey. Ofioliti 40, 73-90.

Fedo, C. M., Sircombe K. N. and Rainbird R. H., 2003. Detrital zircon analysis of the sedimentary record. Reviews in Mineralogy and Geochemistry 53(1), 277-303.

Frassi, C., Göncüoğlu, M.C., Marroni, M., Pandolfi, L., Ruffini, L., Ellero, A., Ottria, G., Sayit, K., 2016. The Intra-Pontide Suture Zone in the Tosya-Kastamonu area, Northern Turkey. Journal of Maps 12, 211-219.

Frassi, C., Marroni, M., Pandolfi, L., Göncüoğlu, M.C., Ellero, A., Ottria, G., Sayit, K., Mcdonald, C.S., Balestrieri, M.L., Malasoma, A., 2018. Burial and exhumation history of the Daday Unit (Central Pontides, Turkey): implications for the closure of the Intra-Pontide oceanic basin. Geological Magazine 155(2), 356-376.

Göncüoğlu, M.C., 2010. Introduction to the Geology of Turkey: Geodynamic evolution of the Pre-Alpine terranes. General Directorate of Mineral. Res. Explor., Monography Series 5, 1-66.

Göncüoğlu, M.C. and Erendil, M., 1990. Pre-Late Cretaceous tectonic units of the Armutlu Peninsula. Proceed. 8th Turkish Petrological Congress 8, 161-168.

Göncüoğlu, M.C., Erendil, M., Tekeli, O., Aksay, A., Kuscu, A., Ürgün, B., 1987. Geology of the Armutlu Peninsula. IGCP-5 Guide Book for the field excursion along Western Anatolia, Turkey, Ankara 5, 12-18.

Göncüoğlu, M.C., Dirik, K. and Kozlu, H., 1997. General Characteristics of Pre-Alpine and Alpine Terranes in Turkey: Explanatory notes to the terrane map of Turkey. Annales Geologique de Pays Hellenique 37, 515-536.

Göncüoğlu, M.C., Gürsu, S., Tekin, U.K., Koksal, S., 2008. New data on the evolution of the Neotethyan oceanic branches in Turkey: Late Jurassic ridge spreading in the Intra-Pontide branch. Ofioliti 33, 153-164.

Göncüoğlu, M.C., Marroni, M., Sayit, K., Tekin, U.K., Ottria, G., Pandolfi, L., Ellero, A., 2012. The Aylı Dağ ophiolite sequence (central-northern Turkey): A fragment of Middle Jurassic oceanic lithosphere within the Intra-Pontide suture zone. Ofioliti 37, 77-91.

Göncüoğlu, M.C., Marroni, M., Pandolfi, L., Ellero, A., Ottria, ö., Catanzariti, R., Tekin, U.K., Sayit, K., 2014. The Arkot Dağ Mélange in Araç area, central Turkey: Evidence of its origin within the geodynamic evolution of the Intra-Pontide suture zone. Journal of Asian Earth Sciences 85, 117-139.

Görür, N., Monod, O., Okay, A.I., Şengör, A.M.C., Tüysüz, O., Yiğitbaş¸ E., Sakinç, M., Akkök, R., 1997. Palaeogeographic and tectonic position of the Carboniferous rocks of the western Pontides (Turkey) in the frame of the Variscan belt. Bulletin de la Société Géologique de France 168, 197-205.

Hippolyte, J.-C., Müller, C., Kaymakci, N., Sangu, E., 2010. Nannoplankton dating in the Black Sea inverted margin of Central Pontides (Turkey) reveals two episodes of rifting. In: Sosson, M., Kaymakci, N., Stephenson, R.A., Bergerat, F., Starostenko, V. (Eds.), Sedimentary Basin Tectonics from the Black Sea and Caucasus to the Arabian Platform, Geologica Society of London, Special Publication 340, pp. 113-136.

Hippolyte, J.-C., Espurt, N., Kaymakci, N., Sangu, E., Müller, C., 2016. Cross-sectional anatomy and geodynamic evolution of the Central Pontide orogenic belt (northern Turkey). International Journal of Earth Sciences 105(1), 81-106.

Jackson, S., 2008. LAMTRACE data reduction software for LA-ICP-MS. In: Sylvester P. (Eds.), Laser ablation-ICP-mass spectrometry in the Earth sciences: Current practices and outstanding issues. Mineralogical Association of Canada Short Course Series 40, 305-307.

Kaygusuz, A., Arslan, M., Siebel, W., Sipah, F., Ilbeyli, N., 2012. Geochronological evidence and tectonic significance of Carboniferous magmatism in the southwest Trabzon area, eastern Pontides, Turkey. International Geology Review 54(15), 1-25.

Machev, P., Ganev, V., Klain, L., 2015. New LA-ICP-MS U-Pb zircon dating for Strandja granites (SE Bulgaria): evidence for two stage late Variscan magmatism in the internal Balkanides. Turkish Journal of Earth Sciences 24, 230-248.

Marroni, M., Frassi, C., Göncüoğlu, M.C., Di Vincenzo, G., Pandolfi, L., Rebay, G., Ellero, A., Ottria, G., 2014. Late Jurassic amphibolite-facies metamorphism in the Intra-Pontide Suture Zone (Turkey): an eastward extension of the Vardar Ocean from the Balkans into Anatolia? Journal of the Geological Society of London 171(5), 605-608.

Moix, P., Beccaletto, L., Kozur, H.W., Hochard, C., Rosselet, F., Stampfli, G.M., 2008. A new classification of the Turkish terranes and sutures and its implication for the paleotectonic history of the region. Tectonophysics 451, 7-39.

Mutti, E., 1992. Turbidite Sandstones. AGIP-Instituto di Geologia, Università di Parma, San Donato Milanese, 275 pp.

Okay, A.I., 1986. High pressure/low temperature metamorphic rocks of Turkey. Geological Society of America Memoir 164, 333-348.

Okay, A.I., 2000. Was the Late Triassic orogeny in Turkey caused by the collision of an oceanic plateau? In: Bozkurt, E., Winchester, J.A., Piper, J.A.D. (Eds.), Tectonics and Magmatism in Turkey and surrounding Area. Geological Society of London, Special Publication 173, 25-41.

Okay, A.I. and Göncüoğlu, M.C., 2004. The Karakaya complex: a review of data and concepts. Turkish Journal of Earth Sciences 13, 77-95.

Okay, A.I. and Topuz, G., 2017. Variscan orogeny in the Black Sea region. International Journal of Earth Sciences (Geol Rundsch) 106, 569-592.

Okay, A.I. and Tüysüz, O., 1999. Tethyan sutures of northern Turkey. In: Durand, B., Olivet, J. L., Horvath, E., Serrane, M. (Eds.), The Mediterranean basins, extension within the Alpine Orogen. Turkish Journal of Earth Sciences 156. pp. 475-515.

Okay, A.I., Satır, M., Maluski, H., Siyako, M., Monie, P., Metzger, R., Akyüz, S., 1996. Paleo- and Neo-Tethyan events in northwest Turkey: geological and geochronological constraints. In: Yin, A., Harrison, M. (Eds.), Tectonics of Asia. Cambridge University Press, pp. 420-441.

Okay, A.I., Monod, O., Monié, P., 2002. Triassic blueschists and eclogites from northwest Turkey: vestiges of the Paleo-Tethyan subduction. Lithos 64, 155-178.

Okay, A.I., Satır, M., Siebel, W., 2006. Pre-Alpide orogenic events in the Eastern Mediterranean region. In: Gee, D.G., Stephenson, R.A. (Eds.), European lithosphere dynamics. Geological Society of London Memoir 32, pp. 389-405.

Okay, A.I., Sunal, G., Sherlock, S., Altıner, D., Tüysüz, O., Kylander-Clark, A.R.C., Aygül, M., 2013. Early Cretaceous sedimentation and orogeny on the active margin of Eurasia: Southern Central Pontides, Turkey. Tectonics 32, 1247-1271.

Okay, A.I., Altiner, D., Sunal, G., Aygül, M., Akdoğan, R., Altiner, S., Simmons, M., 2017. Geological evolution of the Central Pontides. Geological Society of London, Special Publications 464(15), SP464-3.

Ottria, G., Pandolfi, L., Catanzariti, R., Da Prato, S., Ellero, A., Frassi, C., Göncüoğlu, M.C., Marroni, M., Ruffini, L., Sayit, K., 2017. Evolution of an early Eocene pull-apart basin in Central Pontides (Northern Turkey): New insights into the origin of the North Anatolian Shear Zone. Terra Nova 29(6), 392-400.

Ozgül, N., 2012. Stratigraphy and some structural features of the Istanbul Palaeozoic. Turkish Journal of Earth Sciences 21, 817-866.

Plunder, A., Agard, P., Chopin, C., Okay, A.I., 2013. Geodynamics of the Tavşanlı zone, western Turkey: Insights into subduction/obduction processes. Tectonophysics 608, 884-903.

Robertson, A.H.F., 2002. Overview of the genesis and emplacement of Mesozoic ophiolites in the Eastern Mediterranean Tethyan region. Lithos 65, 1-67.

Robertson, A.H.F. and Ustaömer, T., 2004. Tectonic evolution of the Intra-Pontide suture zone in the Armutlu Peninsula, NW Turkey. Tectonophysics 381, 175-209.

Robertson, A.H.F., Clift, P.D., Degnan, P.J., Jones, G., 1991. Palaeogeographical and palaeotectonic evolution of the eastern Mediterranean Neotethys. Palaeogeography, Palaeoclimatology, Palaeoecology 87, 289-343.

Şahin, S.Y., Aysal, N., Güngör, Y., Peytcheva, I., Neubauer, F., 2014. Geochemistry and U-Pb zircon geochronology of metagranites in Istranca (Strandja) Zone, NW Pontides, Turkey: implications for the geodynamic evolution of Cadomian orogeny. Gondwana Research 26, 755-771.

Sayit, K. and Göncüoğlu, M.C., 2013. Geodynamic evolution of the Karakaya Mélange Complex, Turkey: a review of geological and petrological constraints. Journal of Geodynamics 65, 56-65.

Şengör, A.M.C. and Yılmaz, Y., 1981. Tethyan evolution of Turkey: a plate tectonic approach. Tectonophysics 75, 181-241.

Şengör A.M.C., Tüysüz, O., Imren, C., Sakinc, M., Eyidogan, H., Görür, N., Le Pichon, X., Rangin, C., 2005. The North Anatolian Fault: A New Look. Annual Review of Earth and Planetary Sciences 33, 37-112.

Sláma, J., Košler, J., Condon, D.J., Crowley, J.L., Gerdes, A., Hanchar, J.M., Horstwood, M.S.A., Morris, G.A., Basdala, L., Norberg, N., Schaltegger, U., Schoene, B., Tubrett, M.N., Whitehouse, M.J., 2008. Plešovice zircon - A new natural reference material for U-Pb and Hf isotopic microanalysis. Chemical Geology 249, 1-35.

Stampfli, G.M. and Borel, G.D., 2002. A plate tectonic model for the Paleozoic and Mesozoic constrained by dynamic plate boundaries and restored synthetic oceanic isochrons. Earth and Planetary Science Letters 196(1), 17-33.

Stampfli, G.M. and Kozur, H.W., 2006. Europe from the Variscan to the Alpine cycles. In: Gee, D.G., Stephenson, R. (Eds.), European lithosphere dynamics. Geological Society of London Memoirs 32, pp. 57-82.

Sunal, G., 2012. Devonian magmatism in the western Sakarya Zone, Karacabey region, NW Turkey. Geodinamica Acta 25, 183-201.

Sunal, G., Natal'in, B., Satır, M., Toraman, E., 2006. Paleozoic magmatic events in the Strandja Masif, NW Turkey. Geodinamica Acta 19, 283-300.

Tokay, M., 1973. Geological observations on them North Anatolian Fault Zone between Gerede and Ilgaz. Proceedings of the North Anatolian Fault and Earthquakes Symposium, Ankara. The Mineral Research and Exploration Publication, 12-29.

Ulianov, A., Müntener, O., Schaltegger, U., Bussy, F., 2012. The data treatment dipendent variability of U-Pb zircon ages obtained using mono-collector, sector field, laser ablation, ICPMS. Journal of Analytical Atomic Spectrometry 27(4), 663-676.

Ustaömer, P.A. and Rogers, G., 1999. The Bolu Massif: remnant of a pre-Early Ordovician active margin in the West Pontides, northern Turkey. Geological Magazine 136(5), 579-592.

Ustaömer, P.A., Mundil, R., Renne, R., 2005. U/Pb and Pb/Pb zircon ages for arc-related intrusions of the Bolu Massif (W Pontides, NW Turkey): evidence for Late Precambrian (Cadomian) age. Terra Nova 17, 215-223.

Ustaömer, P.A., Ustaömer, T., Robertson, A.H.F., 2012. Ion Probe U-Pb dating of the Central Sakarya basement: a peri-Gondwana Terrane intruded by late Lower Carboniferous subduction/collision-related granitic rocks. Turkish Journal of Earth Sciences 21, 905-932.

Ustaömer, T., Robertson, A.H.F., Ustaömer, P.A., Gerdes, A., Peytcheva, I., 2013. Constraints on Variscan and Cimmerian magmatism and metamorphism in the Pontides (Yusufeli-Artvin area), NE Turkey from U-Pb dating and granite geochemistry. In: Robertson, A.H.F., Parlak, O., Ünlügenç, U.C. (Eds.), Geological development of Anatolia and the easternmost Mediterranean region. Geological Society of London, Special Publication 372, pp. 49-74.

van Hinsbergen, D.J.J., Maffione, M., Plunder, A., Kaymakci, N., Ganerød, M., Hendriks, B.W.H., Corfu, F., Gürer, D., de Gelder, G.I.N.O., Peters, K., McPhee, P.J., Brower, F.M., Advokaat, E.L., Vissers, R.L.M., 2016. Tectonic evolution and paleogeography of Kırşehir Block and the Central Anatolian Ophiolites, Turkey. Tectonics 35, 983-1014.

Yılmaz, Y., 1990. Allochthonous terranes in the Tethyan Middle East, Anatolia and surrounding regions. Philosophical Transaction Royal Society of London 331, 611-624.

Yılmaz, Y., Tüysüz, O., Yiğitbaş, E.C.Ş., Genç, C.Ş., Şengör, A.M.C., 1997. Geology and tectonic evolution of the Pontides. In: Robinson, A.G. (Eds.), Regional and petroleum geology of the Black Sea and surrounding region. American Association of Petroleum Geologists Bulletin 68, pp. 183-226.

CAPTIONS

Fig. 1 - The major tectonic zones of Turkey separated by sutures (thick dotted lines). In red, Neogene to Holocene active regional structures are indicated. The boxed sector indicates the study area.

Fig. 2 - Geology of the study area. a) tectonic scheme of the Daday-Arac-Bayamoren area. Boxed area indicate the location of Fig.2c. b) N-S Geological section of the IPS zone area. c) Close-up of the geology of the study area. The samples location is indicated.

Fig. 3 - Stratigraphic features of the Taraklı Flysch in the study area. a) Reconstructed stratigraphic log of the Taraklı Flysch. The position of the studied samples are indicated in the left side of the log while the pictures position is indicated in the right side. b) Lithofacies legend: 1: slide-block in shaly-matrix; 2: clast supported-conglomerates; 3: coarse-grained turbidites; 4: medium-grained arenites; 5: thin-bedded turbidites. c-g) Field occurrence of the Taraklı Flysch in the Bahcecik area. c) Thin Bedded Turbidites lithofacies; d) level of well rounded clast- to matrix-supported conglomerates (arrows) associated with coarse-grained arenites. e) well-rounded matrix-supported conglomerates showing several granitoids clasts. f) slide-blocks of Permian granitoids. g) slide-blocks of Permian granitoids (arrow) and crinoidal Devonian-Carboniferous limestones.

Fig. 4 - Field occurence and photomicrographs of the study rocks. a) and b) Quartz-monzonites (TC316). c) and d) leucocratic granodiorites (TC319). e) cm and f) mm leucocratic granodiorites veinlet intruding quartz-monzonites. The arrows indicate the magmatic relationships.

Fig. 5 - Zircon CL images and analysis points of the samples a) TC316a, b) TC316b and c) TC319. In blue are indicated the spots whose value has been used to calculate the

weighted average age of the samples; green color has been used for the spots whose value has been used to calculate the weighted average age and that is included within the error of the sample age. In red are marked the spots whose age has not been considered for the age calculation.

Fig. 6 - Concordia diagrams of TC316a and TC319 samples and weighted average diagrams of the three samples TC316a, TC316b and TC319.

Fig. 7 - 3D reconstruction of the Taraklı Flysch depositional system and surrounding areas during the Late Cretaceous-Middle Paleocene time. The setting of the study granitoids are indicated as part of IZ zone as well as slide-block in the inner foredeep of the Taraklı basin.

Table 1 - Results of zircon LA-ICP-MS U-Pb age determination of the samples TC316a, TC316b, TC319. The results related to the secondary standard "Plešovice" is also reported.

Figure 1

Click here to download high resolution image

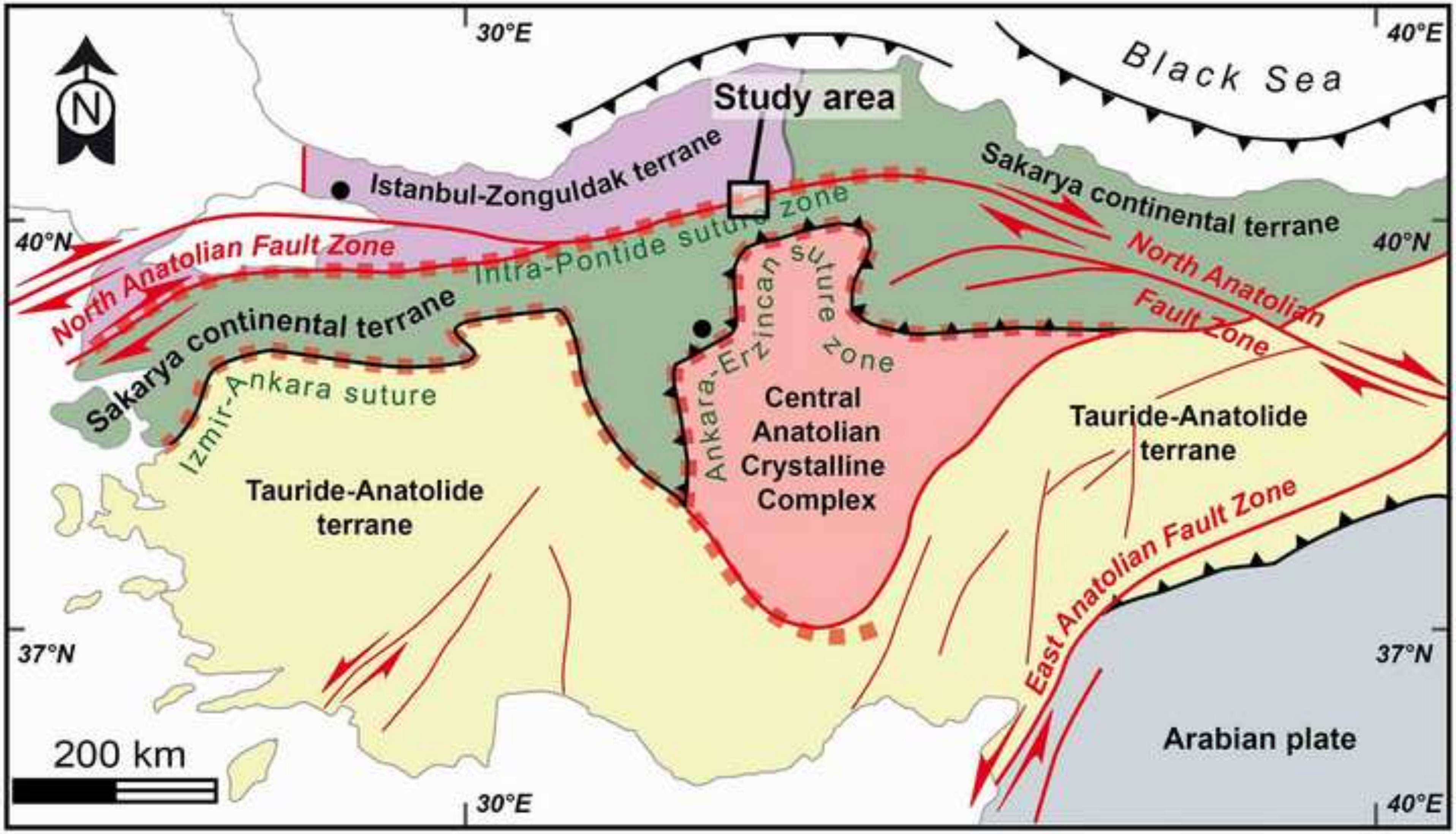

Figure 2
Click here to download high resolution image

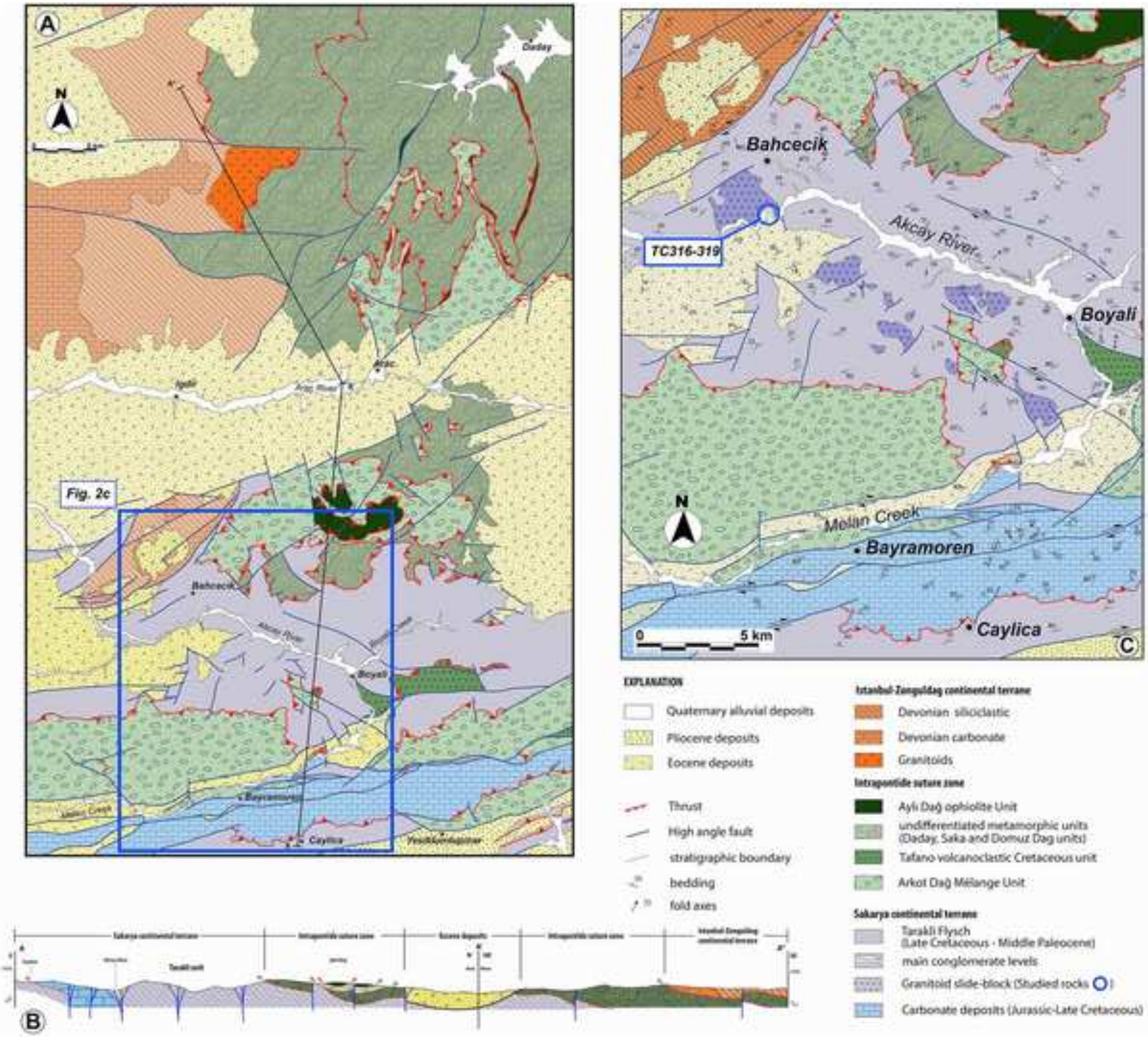

Figure 3

Click here to download high resolution image

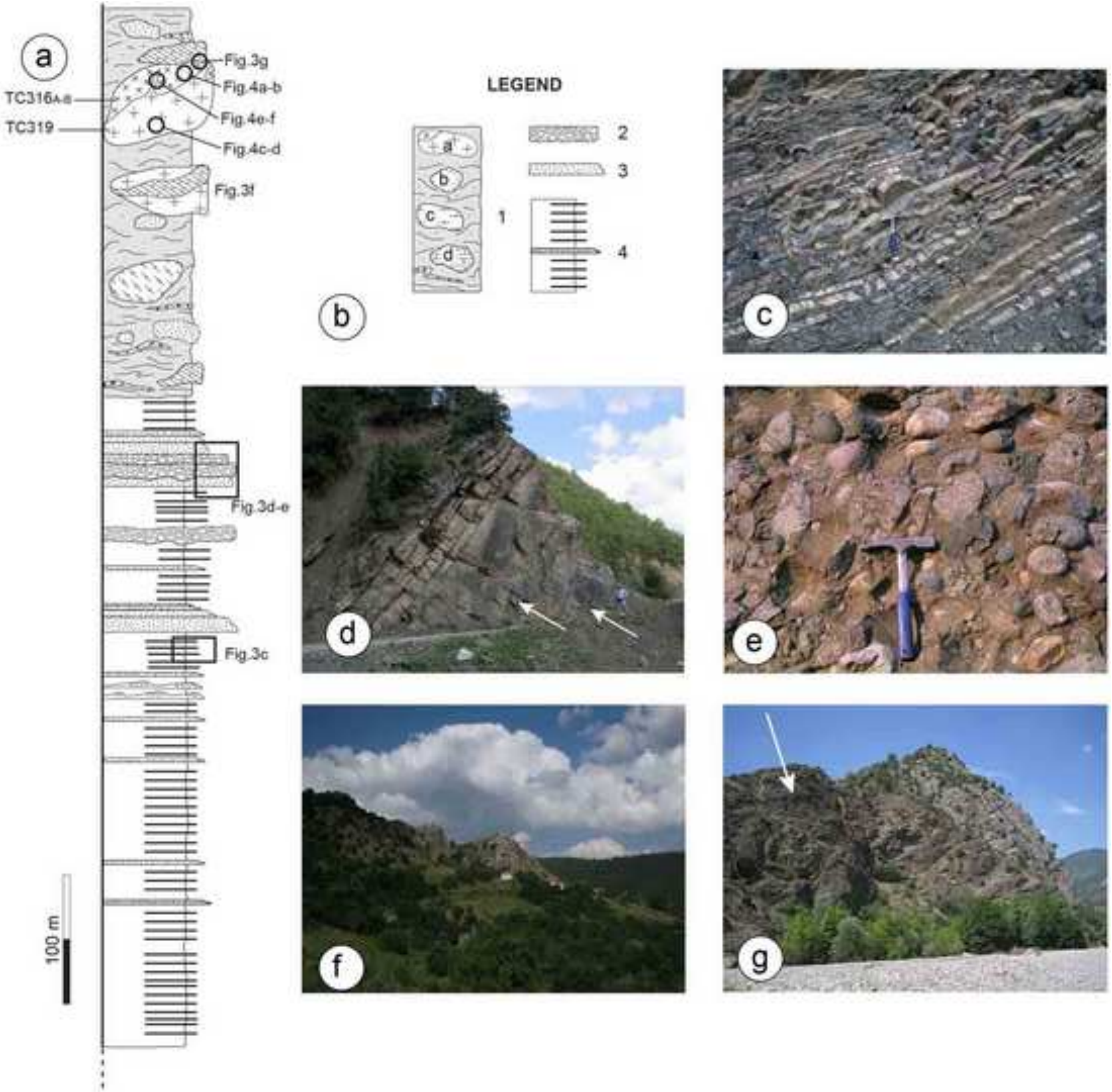

Figure 4
Click here to download high resolution image

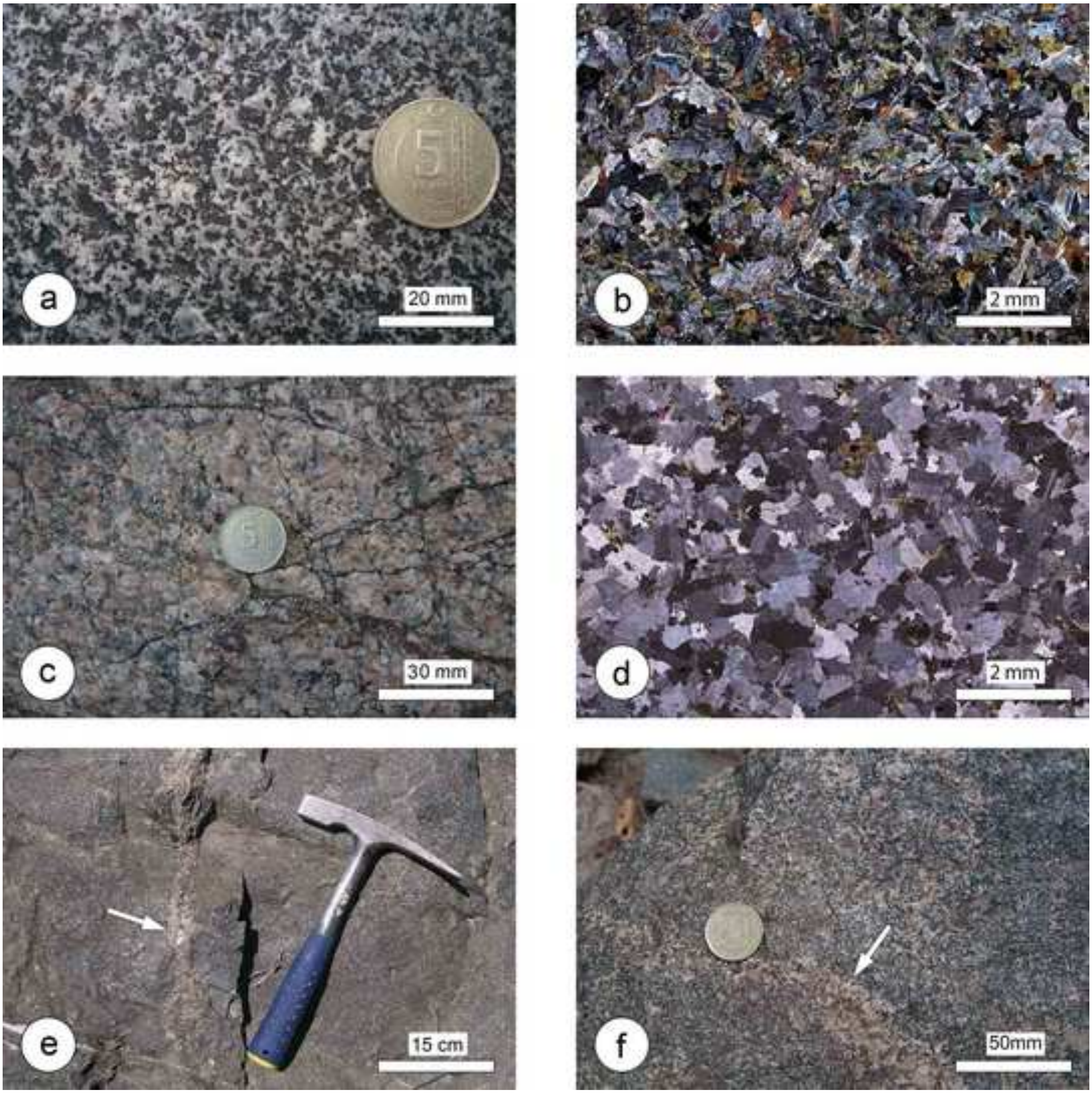

Figure 5

Click here to download high resolution image

Figure 6
Click here to download high resolution image

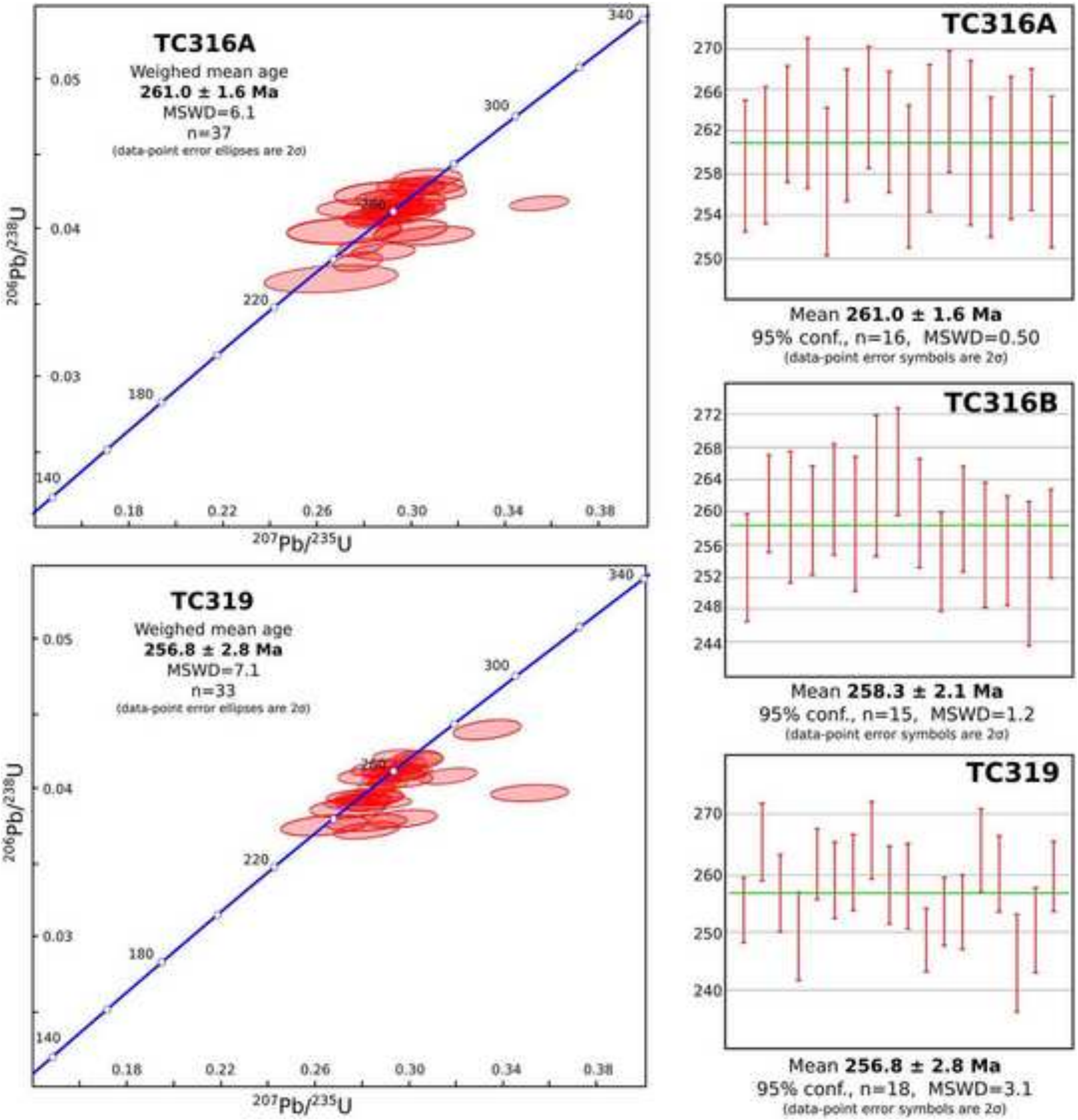

Figure 7
Click here to download high resolution image

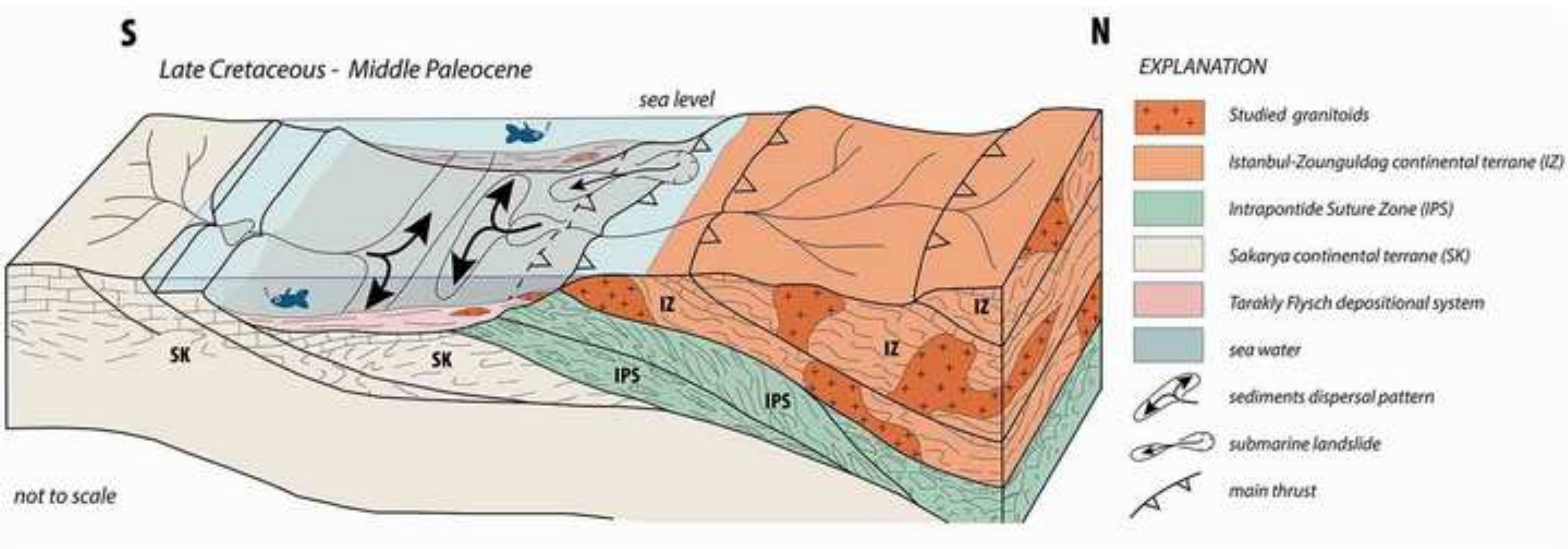

Table 1

zircon	Isotopic ratios				ρ	Age (Ma)		Apparent ages (Ma)				Conc.(%)
	$^{206}Pb/^{238}U$	2S.D.	$^{207}Pb/^{235}U$	2S.D.		$^{206}Pb/^{238}U$	S.D.	$^{207}Pb/^{235}U$	S.D.	$^{207}Pb/^{206}Pb$	S.D.	
TC316A												
jn11n05	0.041	0.0003936	0.2905	0.008	0.34	258.8	2.4	258.9	6.4	270	54	95.9
jn11n06	0.0411	0.00040278	0.2928	0.008	0.37	259.7	2.5	260.7	6.1	300	56	86.6
jn11n08	0.0416	0.00034112	0.2922	0.006	0.41	262.8	2.1	260.3	4.5	274	40	95.9
jn11n09	0.0399	0.00035112	0.2903	0.005	0.53	252	2.2	258.8	3.8	322	34	78.3
jn11n10	0.0418	0.00043472	0.3031	0.010	0.32	263.8	2.7	268.8	7.7	332	66	79.5
jn11n11	0.0407	0.00047212	0.2932	0.012	0.29	256.9	2.9	261.1	9.3	306	86	84.0
jn11n12	0.0378	0.00050652	0.2768	0.009	0.42	239.2	3.1	248.1	7	338	64	70.8
jn11o05	0.0418	0.00035112	0.3015	0.006	0.40	264.3	2.2	267.6	5	304	46	86.9
jn11o06	0.0428	0.00041944	0.3042	0.009	0.34	270.4	2.6	269.7	6.8	304	56	88.9
jn11o09	0.0408	0.00042432	0.2864	0.010	0.31	257.8	2.6	255.7	7.7	266	72	96.9
jn11o12	0.0388	0.0004656	0.2783	0.008	0.41	245.3	2.9	249.3	6.5	290	60	84.6
jn11o13	0.0414	0.00043884	0.3051	0.008	0.42	261.4	2.7	270.4	6	368	48	71.0
jn11o14	0.0366	0.00076128	0.2666	0.022	0.25	232	4.8	240	17.7	326	188	71.2
jn11t10	0.0418	0.00035112	0.2961	0.005	0.49	264	2.2	263.4	3.9	272	36	97.1
jn11t12	0.0413	0.00047908	0.2997	0.013	0.28	261	3	266.2	9.8	296	90	88.2
jn11v05	0.0399	0.00075012	0.2815	0.028	0.19	252.1	4.7	251.9	22.5	308	184	81.9
jn11v06	0.041	0.0004182	0.3007	0.009	0.35	258.7	2.6	266.9	6.9	338	60	76.5
jn11v07	0.0412	0.00042024	0.2964	0.009	0.34	260.5	2.6	263.6	7	306	62	85.1
jn11v08	0.0414	0.00042228	0.3041	0.008	0.37	261.3	2.6	269.6	6.5	354	56	73.8
jn11v09	0.0408	0.00045696	0.2846	0.011	0.28	258.1	2.8	254.3	9	282	86	91.5
jn11v13	0.0426	0.00039192	0.3068	0.008	0.35	269.2	2.4	271.7	6.3	290	52	92.8
TC316B												
jn11e05	0.04	0.00042	0.287	0.010	0.29	253.1	2.6	256.2	8	288	74	87.9
jn11e06	0.0413	0.00038	0.3006	0.008	0.34	261	2.3	266.9	6.4	332	52	78.6
jn11e08	0.0435	0.00051	0.3088	0.017	0.22	274.4	3.2	273.3	12.8	272	104	100.9
jn11e09	0.041	0.000418	0.2939	0.010	0.30	259	2.6	261.6	7.9	314	66	82.5
jn11e11	0.0414	0.00041	0.2988	0.010	0.29	261.5	2.6	265.4	8.1	276	72	94.7
jn11e12	0.0409	0.00052	0.2987	0.015	0.24	258.5	3.2	265.4	12	352	102	73.4
jn11e14	0.0422	0.00041	0.2977	0.010	0.29	266.2	2.5	264.6	7.7	262	70	101.6
jn11f05	0.0411	0.000411	0.2933	0.009	0.34	259.8	2.6	261.2	6.7	280	62	92.8
jn11f06	0.0402	0.00039	0.2815	0.009	0.30	253.9	2.4	251.8	7	264	66	96.2
jn11f07	0.041	0.000402	0.2932	0.008	0.34	259.1	2.5	261.1	6.6	294	56	88.1
jn11f09	0.0405	0.00049	0.2949	0.012	0.30	255.9	3	262.4	9.3	300	78	85.3
jn11f10	0.0404	0.00042	0.292	0.011	0.27	255.2	2.6	260.2	8.7	316	76	80.8
jn11f12	0.0407	0.00034	0.2954	0.006	0.42	257.3	2.1	262.8	4.6	308	42	83.5
jn11f13	0.04	0.00038	0.2811	0.009	0.31	253	2.3	251.5	6.8	248	60	102.0
jn11f14	0.0394	0.00039	0.274	0.007	0.37	248.9	2.4	245.9	5.7	240	56	103.7
TC319												
jn11p05	0.0401	0.0003609	0.2908	0.006	0.41	253.7	2.2	259.2	5.1	338	46	75.1
jn11p06	0.042	0.0004032	0.3036	0.009	0.33	265.3	2.5	269.2	6.8	304	62	87.3
jn11p07	0.0406	0.00041412	0.2981	0.010	0.31	256.6	2.6	264.9	7.6	342	64	75.0
jn11p09	0.0394	0.00048856	0.2765	0.010	0.36	249.2	3	247.9	7.6	272	72	91.6
jn11p10	0.0414	0.00036432	0.2951	0.007	0.35	261.6	2.3	262.5	5.8	292	54	89.6
jn11p12	0.041	0.00041	0.2964	0.008	0.38	258.8	2.5	263.6	6.1	306	56	84.6

jn11p13	0.0439	0.0005268	0.3333	0.011	0.35	277	3.2	292.1	8.7	420	70	66.0
jn11q05	0.0412	0.00040376	0.2866	0.009	0.30	260.1	2.5	255.9	7.4	298	58	87.3
jn11q06	0.0421	0.00040416	0.295	0.009	0.32	265.6	2.5	262.5	7	258	60	102.9
jn11q14	0.039	0.0004524	0.2822	0.015	0.22	246.3	2.8	252.4	11.9	352	104	70.0
jn11t05	0.0408	0.0004488	0.2952	0.010	0.31	257.8	2.8	262.7	8.2	290	70	88.9
jn11t06	0.0393	0.00036156	0.2883	0.008	0.32	248.6	2.2	257.3	6.5	326	58	76.3
jn11z05	0.0377	0.00055796	0.2813	0.014	0.29	238.3	3.4	251.7	11.5	352	110	67.7
jn11z06	0.0401	0.00036892	0.287	0.008	0.35	253.4	2.3	256.2	6	286	60	88.6
jn11z07	0.0401	0.00039298	0.2873	0.009	0.30	253.3	2.5	256.5	7.3	300	70	84.4
jn11z08	0.0418	0.00043472	0.3048	0.008	0.40	264	2.7	270.1	6.2	320	54	82.5
jn11z09	0.0411	0.00039456	0.2907	0.009	0.30	259.9	2.5	259.1	7.2	260	64	100.0
jn11z10	0.0387	0.0005418	0.2737	0.013	0.29	244.7	3.4	245.6	10.5	294	102	83.2
jn11z11	0.0375	0.0006	0.2647	0.016	0.27	237.5	3.7	238.5	12.8	264	130	90.0
jn11z12	0.0396	0.00045936	0.2819	0.011	0.29	250.2	2.9	252.2	8.8	242	84	103.4
jn11z13	0.0411	0.00037812	0.2988	0.009	0.32	259.5	2.3	265.5	6.7	332	58	78.2
Plešovice												
ples-a15	0.0535	0.000417	0.4025	0.008	0.39	335.9	2.6	343.5	5.8	392	40	85.7
ples-b15	0.054	0.000421	0.3954	0.008	0.39	338.8	2.6	338.3	5.8	330	40	102.7
ples-b16	0.0538	0.000463	0.3957	0.009	0.38	337.8	2.8	338.5	6.5	334	46	101.1
ples-c15	0.054	0.000432	0.4008	0.007	0.43	339	2.7	342.2	5.4	356	38	95.2
ples-d15	0.0536	0.000429	0.4008	0.010	0.33	336.9	2.6	342.2	7.1	372	50	90.6
ples-e16	0.0536	0.00045024	0.4031	0.009	0.36	336.3	2.7	343.9	6.8	378	44	89.0
ples-f16	0.0538	0.0004842	0.3915	0.009	0.40	337.9	2.9	335.4	6.5	322	46	104.9
ples-h15	0.054	0.000454	0.3924	0.009	0.35	339.1	2.8	336.1	6.9	318	50	106.6
ples-i15	0.0537	0.000462	0.4098	0.010	0.37	337.1	2.8	348.8	6.9	402	44	83.9
ples-i16	0.0537	0.000473	0.3991	0.011	0.33	337.4	2.9	341	7.6	348	50	97.0
ples-m15	0.0536	0.000461	0.3847	0.007	0.45	336.9	2.8	330.5	5.4	312	40	108.0
ples-m16	0.0539	0.000464	0.4001	0.008	0.41	338.7	2.8	341.7	6.1	356	42	95.1
ples-n16	0.0537	0.00047256	0.4011	0.008	0.43	337.3	2.9	342.5	5.9	382	38	88.3
ples-o16	0.0538	0.00045192	0.3964	0.008	0.42	337.6	2.8	339	5.8	348	44	97.0
ples-p15	0.0539	0.00044198	0.3952	0.008	0.41	338.2	2.7	338.2	5.7	344	38	98.3
ples-r15	0.054	0.000475	0.4062	0.009	0.42	339.1	2.9	346.2	6.2	354	38	95.8
ples-t15	0.0535	0.0004387	0.3993	0.008	0.39	336.1	2.7	341.1	6.1	378	40	88.9
ples-t16	0.054	0.000486	0.3937	0.010	0.37	338.9	2.9	337.1	7	338	50	100.3
ples-u16	0.0537	0.000451	0.3946	0.008	0.42	336.9	2.7	337.7	5.7	350	42	96.3
ples-v15	0.0535	0.0004815	0.3905	0.008	0.42	336	3	334.7	6.1	338	42	99.4
ples-z16	0.0535	0.0004922	0.404	0.009	0.42	335.8	3	344.5	6.4	386	40	87.0